



Anti-liver fibrosis effect of total flavonoids from *Scabiosa comosa* Fisch. ex Roem. et Schult. on liver fibrosis in rat models and its proteomics analysis

Menggensilimu^{1#}, Hongwei Yuan^{2#}, Chunmei Zhao^{3#}, Xiaomei Bao⁴, Haisheng Wang⁵, Jie Liang¹, Yuxin Yan¹, Chunyan Zhang¹, Rong Jin¹, Lijie Ma¹, Jianyu Zhang⁵, Xiaoli Su⁶, Yuehong Ma¹

¹Department of Pharmacology, ²Department of Pathology, School of Basic Medicine, Inner Mongolia Medical University, Hohhot City 010107, China; ³Department of Nephrology, The Affiliated Hospital of Inner Mongolia Medical University, Hohhot City 010107, China; ⁴Department of Pharmaceutical Engineering, School of Pharmacy, ⁵Department of Biochemistry, School of Basic Medicine, ⁶Functional Science laboratory, Institute of Basic Medicine, Inner Mongolia Medical University, Hohhot City 010107, China

Contributions: (I) Conception and design: Y Ma, Menggensilimu; (II) Administrative support: Y Ma, H Yuan, C Zhao; (III) Provision of study materials or patients: H Yuan; (IV) Collection and assembly of data: X Bao; (V) Data analysis and interpretation: H Wang; (VI) Manuscript writing: All authors; (VII) Final approval of manuscript: All authors.

[#]These authors contributed equally to this work.

Correspondence to: Yuehong Ma. Department of Pharmacology, School of Basic Medicine, Inner Mongolia Medical University, Hohhot City 010107, China. Email: myh19982002@sina.com.

Background: To explore the potential therapeutic effect of total flavonoids (TFs) extracted from *Scabiosa comosa* Fisch. ex Roem. et Schult on liver fibrosis in rat models and to identify the possible targets and pathways of TF in treating liver fibrosis by using a quantitative proteomics method.

Methods: Sixty Wistar rats were equally randomized into five groups: a blank control group, a model group, and high-, intermediate-, and low-dose TF treatment groups. Except for the blank control group, rats in the other four groups were intragastrically administered with CCL4 2 mL/kg to establish the liver fibrosis models. Furthermore, the high-, intermediate-, and low-dose TF groups were intragastrically given TF at a dose of 200, 100 and 50 mg/kg, respectively. After 10 weeks, the rats were sacrificed, and blood and liver samples were collected. Serum alanine transaminase (ALT), Aspartate aminotransferase (AST), and alkaline phosphatase (ALP) levels were measured, and hematoxylin and eosin (HE) staining and Masson's trichrome staining were used to observe the pathological changes in each group. The hydroxyproline content was also determined. Real-time polymerase chain reaction (PCR) and Western blotting (WB) were performed to detect the mRNA and protein expressions of α -smooth muscle actin (α SMA) and Collagen I. Mass spectrometry was performed for proteomic analysis.

Results: Compared with the blank control group, the model group had significantly higher ALT, AST, ALP, and hydroxyproline levels; also, HE and Masson staining showed fibrotic lesions and inflammatory cell infiltration in the model group. Compared with the model group, the high-, intermediate-, and low-dose TF groups had significantly decreased ALT, AST, and ALP levels ($P < 0.05$), and a significantly lower hydroxyproline level ($P < 0.05$), along with remarkably improved fibrotic lesions and inflammatory cell infiltration. Real-time PCR and WB showed that the model group had significantly higher expressions of α SMA and collagen I than those in the blank control group, whereas the TF groups had significantly lower expressions of α SMA and collagen I than those in the model group. A total of 5,014 proteins were detected by quantitative proteomics, among which 205 proteins were differentially expressed, 77 of which were up-regulated and 128 of which were down-regulated. KEGG pathway analysis indicated that the peroxisome proliferator activated receptor (PPAR) and ECM-receptor interaction pathways were down-regulated in the TF groups compared with the model group. Among them, fatty-acid-binding protein (FABP) and von Willebrand factor (vWF) were the key proteins in the PPAR and extracellular matrix (ECM)-receptor interaction pathways. The proteomic results were validated by using WB, yielding consistent results.

Conclusions: Our result demonstrated that the TF extract of *Scabiosa comosa* Fisch. ex Roem. et Schult has a good anti-liver fibrosis effect and may prevent liver fibrosis by reducing the content of α -SMA, CollagenI in liver tissue. The anti-fibrosis mechanism of TF extract of *Scabiosa comosa* Fisch. ex Roem. et Schult may be the inhibition of key proteins FABP and vWF in PPAR, ECM RECEPTOR INTERACTION pathway.

Keywords: Liver fibrosis; total flavonoids (TFs); *Scabiosa comosa* Fisch. ex Roem. et Schult.; proteomics; peroxisome proliferator activated receptor (PPAR); ECM-receptor interaction (extracellular matrix-receptor interaction)

Submitted Nov 11, 2019. Accepted for publication Feb 04, 2020.

doi: 10.21037/apm.2020.02.29

View this article at: <http://dx.doi.org/10.21037/apm.2020.02.29>

Introduction

Liver fibrosis is a pathological process characterized by an abnormal increase and excessive deposition of extracellular matrix (ECM) in the liver during the repair of liver damage and inflammation caused by a variety of pathogenic factors. It is a common pathological feature of most chronic liver diseases and also a key intermediate link during the progression of various chronic liver diseases towards cirrhosis. It is currently believed that liver fibrosis is reversible while cirrhosis is irreversible, and therefore it is important to treat liver fibrosis in a timely fashion before it progresses towards the cirrhotic stage (1). Among the possible treatments, natural products typically have diverse structures, low toxicity, and wide availability and thus may play a unique role in managing fibrosis. *Scabiosa comosa* Fisch. ex Roem. et Schult. is a unique medicinal plant in traditional Mongolian medicine and also a key component in various formulas used by traditional Mongolian medicine to treat liver diseases (2-7). Based on a literature review and the results of our previous experiments, we extracted the total flavonoids (TFs) from *Scabiosa comosa* Fisch. ex Roem. et Schult. and investigated its potential anti-fibrotic effect. TF has multiple components and acts on multiple pathways and targets. Proteins have many different and varied biological functions and play key roles in the onset of liver fibrosis. The successful application of the rapid and high-throughput proteomics technology in drug screening provides an effective approach for identifying drug targets with multiple components. In our current study, we measured the serum biochemical markers, observed histopathological specimens, and completed pharmacodynamic studies by using real-time fluorescence-based quantitative polymerase chain reaction (PCR) and Western blotting (WB); in addition, the differentially expressed proteins in the liver fibrosis model group and TF treatment groups were analyzed by using

serum proteomic analysis with tandem mass tags (TMT), and the results were validated by bioinformatic analysis and WB. It is expected that the findings of this study might produce a basis for treating liver fibrosis with TF from *Scabiosa comosa* Fisch. ex Roem. et Schult.

Methods

Reagents and equipment

The TF powder was self-made. It was dissolved in 0.5% sodium carboxymethylcellulose solution to make a suspension, which was intragastrically administered in rat models. The sodium carboxymethylcellulose was purchased from Tianjin Yongsheng Fine Chemicals. Co., Ltd.; carbon tetrachloride was purchased from Sinopharm Chemical Reagent Co., Ltd.; alanine transaminase (ALT), aspartate aminotransferase (AST), alkaline phosphatase (ALP), and hydroxyproline assay kits were purchased from Nanjing Jianjian (China, Nanjing); the Trizol FastKing cDNA first-strand synthesis kit, and SuperReal PreMix (SYBR Green) kit were purchased from Beyotime (Beijing, China); phenylmethylsulfonyl fluoride (PMSF), sodium dodecyl sulfate (SDS), glycine (Gly), and Tween-20 (Tween-20) were purchased from Solarbio (Beijing, China); trimethylolaminomethane (Tris), RIPA lysis buffer, BCA protein assay kit, and blocking solution were purchased from Beyotime (Beijing, China); rabbit anti-mouse polyclonal antibody was purchased from Proteintech (Wuhan, China); and goat anti-rabbit fluorescently-labeled secondary antibody was purchased from Abbkine.

Animal modeling and treatment

Sixty adult SPF Wistar rats weighing about 220 g were

purchased from Charles River Laboratories (Beijing, China). All animals were adaptively fed for 1 week and then randomized into five groups including the blank control group, model group, and the high-, intermediate-, and low-dose TF treatment groups, with 12 rats in each group. The experiment was performed at the Experimental Animal Center of Inner Mongolia Medical University. The relative humidity of the animal breeding environment was 30–40%, and the relative temperature was 18–24 °C. Natural lighting was offered. Diets were the same for all animal groups, and the rats were fed and watered ad libitum. All the animal feeds and bedding were purchased from the Experimental Animal Center of Inner Mongolia Medical University.

Except for the blank control group, modeling was performed in the remaining four groups by intragastric administration of 50% CCL4 2 mL/kg twice weekly (on the morning of Tuesday and Friday). Furthermore, the high-, intermediate-, and low-dose TF groups were administered with TF suspension at a dose of 200, 100 and 50 mg/kg, respectively. The experiment lasted 10 weeks. The rats were sacrificed under anesthesia on the 10th week. Blood samples were collected for serum biochemical tests. Liver tissue was harvested and weighed, and the liver coefficient was calculated. One part of the liver tissue was fixed in a 10% formaldehyde solution for histological observation, and the remaining parts were preserved in a –80 °C refrigerator for subsequent use (8).

Measurement of serum biochemical markers

After serum was separated from blood, three liver function indicators including serum ALT, AST, and ALP were determined according to the kit instructions.

Determination of hydroxyproline in liver tissue

Liver tissue with a wet weight of 30–100 mg was used for determining the hydroxyproline content according to the kit instructions. The formula for content calculation was as follows: hydroxyproline content (µg/mg wet weight) = (measured OD value – blank OD value)/(standard OD value – blank OD value) × standard concentration (5 µg/mL) × total hydrolysate volume (10 mL/tissue wet weight (mg)).

Histopathological test

The liver tissue was fixed in 10% formaldehyde, embedded

in paraffin, and then cut into 5 µm-thick slices for HE and Masson staining. All the sections were scanned with a Leica digital pathology platform.

Proteomic analysis

Sample preparation and labeling with TMT reagents

The sample was obtained from a –80 °C refrigerator. An appropriate amount of tissue sample was weighed and put into a mortar precooled with liquid nitrogen, in which liquid nitrogen was added to grind the tissue into a fine powder. Samples from each group were mixed with lysis buffer at a volume equal to 20 times and lysed by ultrasound. The product was centrifuged at 12,000 rpm for 10 min at 4 °C. After the cell debris was removed, the supernatant was transferred to a new centrifuge tube, where the protein concentration was determined by using the BCA kit.

Dithiothreitol was added to the protein solution to a final concentration of 5 mM, which was reduced at 56 °C for 30 min. Subsequently, iodoacetamide was added to a final concentration of 11 mM, and the mixture was incubated at room temperature for 15 min in the dark. Finally, the urea concentration of the sample was diluted to below 2 M. Trypsin was added at a mass ratio of 1:50 (trypsin:protein) and digested overnight at 37 °C. Then, trypsin was added again at a mass ratio of 1:10 AM (trypsin:protein) and digested for an additional 4 hours.

Trypsinized peptides were desalted with StrataXC18 (Phenomenex) and lyophilized in vacuo. The peptides were dissolved with 0.5 M of TEAB and labeled according to the instructions of the TMT kit. Specifically, the labeling reagent was thawed and then dissolved with acetonitrile; it was mixed with the peptide and the mixture was incubated at room temperature for 2 hours. The labeled peptides were mixed before they were desalted and then lyophilized in vacuo.

Mass spectrometry

The peptides were fractionated by high-pH reverse high-performance liquid chromatography (HPLC), and the Agilent 300Extend C18 Column (particle diameter, 5 µm; inner diameter, 4.6 mm; and length, 250 mm) was used. After the peptides were separated by an ultra-high-performance liquid system, they were injected into a nanospray ionization (NSI) ion source for ionization and then analyzed by Orbitrap Fusion Lumos mass spectrometry.

Database search

The secondary ion mass spectrometry (SIMS) data were searched in Maxquant version 1.5.2.8. Gene Ontology (GO) analysis was divided into three categories: biological processes, cellular components, and molecular functions. Fisher's exact test was used to test differentially expressed proteins against the background of the identified proteins, and a P value of less than 0.05 was considered statistically significant in the GO enrichment analysis. The Kyoto Encyclopedia of Genes and Genomes (KEGG) database was used for pathway enrichment analysis. Fisher's exact test was used to test differentially expressed proteins against the background of the identified proteins, and a P value of less than 0.05 was considered statistically significant in the pathway enrichment analysis. Finally, these pathways were classified according to the KEGG pathway classification method.

The InterPro database was used to analyze the enrichment of functional domains of differentially expressed proteins. Fisher's exact test was used to test differentially expressed proteins against the background of the identified proteins, and a P value of less than 0.05 was considered statistically significant in the domain unit enrichment analysis.

Cluster analysis based on functional enrichment of differentially expressed proteins (or differentially expressed proteins with different multiples) in different groups was used to study their potential relationships and differences in specific functions (GO, KEGG pathway, protein domain, etc.).

The differentially expressed protein identifiers or protein sequences identified in different groups were compared with the STRING (v.10.5) protein-protein interaction networks, and then the differentially expressed protein interaction relationships were extracted based on a confidence score of >0.7 (high confidence). Finally, the R package "networkD3" tool was used to visualize the differentially expressed protein-protein interaction networks.

WB

Hepatic tissue total protein was extracted with RIPA lysis solution containing 1 mM of PMSF. The protein concentration was measured with the BCA protein assay kit. An equal volume of protein sample was used for sodium dodecyl sulfate polyacrylamide gel electrophoresis (SDS-PAGE), and the products were transferred to a nitrocellulose (NC) membrane. They were blocked with

WB blocking solution for 15 min at room temperature and then incubated with the primary antibody at 4 °C overnight. After washing with tris-buffered saline with Tween 20 (TBST), they were fluorescently labeled and incubated with the secondary antibody at room temperature for 1 hour. After washing with TBST, the products were scanned using the Odyssey[®] Infrared Imaging System, with GAPDH as the internal reference.

Quantitative real-time polymerase chain reaction (qRT-PCR)

The total RNA in liver tissue was extracted by using the Trizol method. Reverse transcription was performed using the FastKing cDNA first-strand synthesis kit. Quantitative detection was performed on the Applied Biosystems[®] 7500 Fast Dx Real-Time PCR Instrument using a SuperReal PreMix kit. The upstream and downstream primer sequences used were as follows:

Collegan I Forward: TGTTGGTCCTGCTGGCAAGAATG
Reverse: GTCACCTTGTTTCGCCTGTGCGCAGC
 α -smooth muscle actin (α SMA) Forward:
GCGTGGCTATTTCCTTCGTGACTAC
Reverse: CCATCAGGCAGTTCGTAGCTCTTC

Statistical analysis

All data were analyzed and processed using the SPSS software package version 19.0. Data of each group are presented as mean \pm standard deviation ($\bar{x} \pm SD$). For data following a normal distribution with uniform variance, one-way analysis of variance (ANOVA) was applied; for heterogeneous data that were not normally distributed, the rank-sum test was performed. A P value of 0.05 was considered to be statistically significant.

Results

Therapeutic effect of TF from Scabiosa comosa Fisch. ex Roem. et Schult. on liver fibrosis

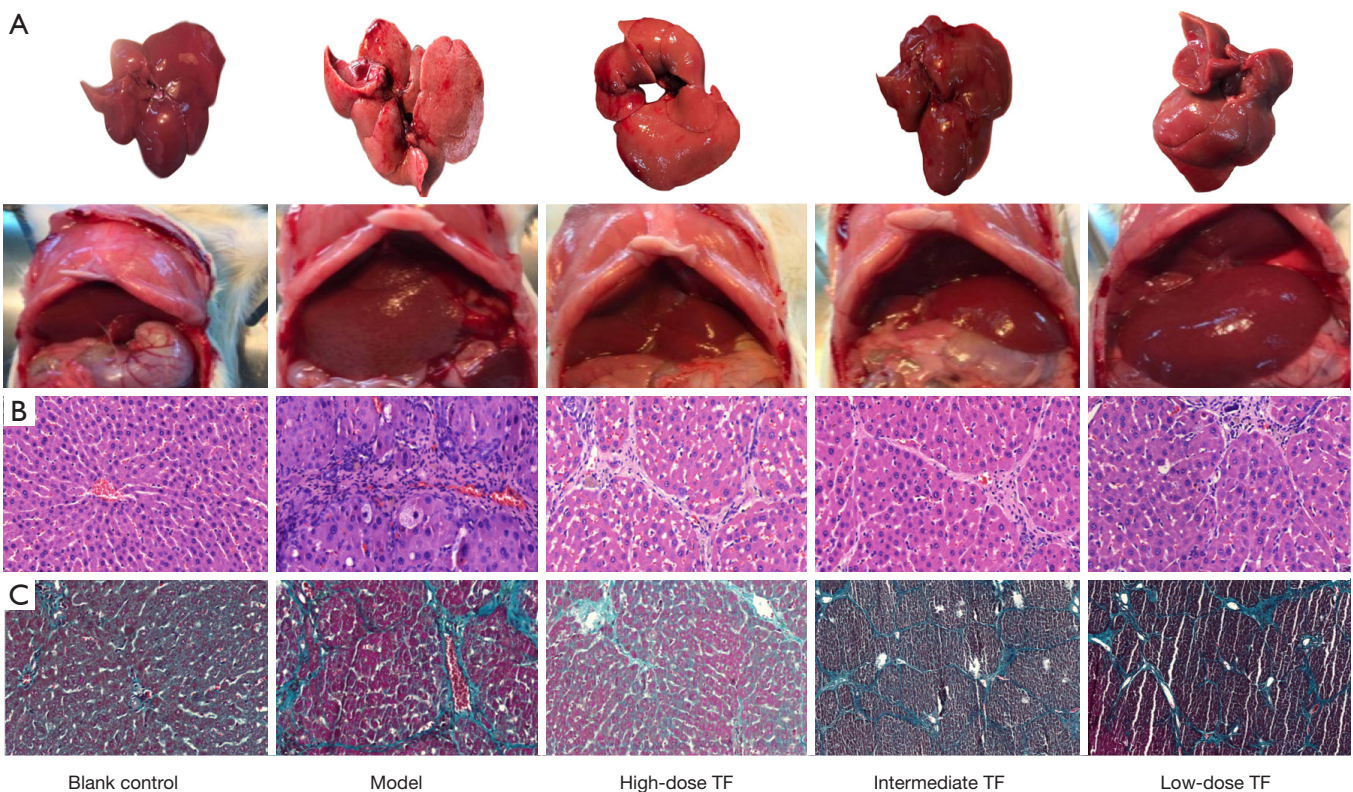
Serum biochemical markers

The measurement results of serum biochemical markers are summarized in *Table 1*. Compared with the blank control group, the model group had significantly higher ALT, AST, and ALP levels (all $P < 0.05$); compared with the model group, while the TF groups had significantly decreased ALT, AST, and ALP levels (all $P < 0.05$).

Table 1 Effects of total flavonoids from *Scabiosa comosa* Fisch. ex Roem. et Schult. on serum biochemical indicators, hydroxyproline content, and liver coefficient in liver fibrosis rats ($\bar{x}\pm s$)

| Group | n | ALT (U/L) | AST (U/L) | AKP (U/L) | Hydroxyproline ($\mu\text{g/g}$) | Liver coefficient |
|----------------------------|----|--------------------------------|---------------------------------|---------------------------------|-------------------------------------|--------------------------------|
| Blank control group | 10 | 9.82 \pm 5.56 | 15.65 \pm 4.67 | 15.46 \pm 6.58 | 333 \pm 49.41 | 3.06% \pm 0.22% |
| Model group | 10 | 33.63 \pm 8.40 ^{##} | 36.41 \pm 17.06 ^{##} | 46.58 \pm 24.85 ^{##} | 1,228.95 \pm 175.06 ^{##} | 3.97% \pm 0.54% [#] |
| High-dose TF group | 10 | 19.35 \pm 9.01 ^{**} | 30.35 \pm 13.50 | 23.52 \pm 12.99 [*] | 837.36 \pm 272.84 ^{**} | 3.18% \pm 0.24% [*] |
| Intermediate-dose TF group | 10 | 14.50 \pm 6.34 ^{**} | 19.24 \pm 7.53 ^{**} | 16.21 \pm 14.83 ^{**} | 834.34 \pm 221.90 ^{**} | 3.47% \pm 0.30% [*] |
| Low-dose TF group | 10 | 15.56 \pm 8.12 ^{**} | 27.51 \pm 11.95 | 11.40 \pm 7.32 ^{**} | 1,048.80 \pm 392.22 | 3.33% \pm 0.31% [*] |

[#], P<0.05, ^{##}, P<0.01, compared with the blank control group; ^{*}, P<0.05, ^{**}, P<0.01, compared with the model group.

**Figure 1** Appearance and pathology of liver tissue. (A) *In vivo* and *ex vivo* livers; (B) H&E staining ($\times 20$); (C) Masson staining ($\times 20$).

Pathological findings

To further confirm the efficacy, we observed the liver morphology and pathology *in vivo*. The morphologies of the *in vivo* livers and fresh livers showed that the livers were smooth, bright red, and soft in the blank control group, while they were rough, yellow or dark-red, and hard in texture in the model group; however, these characteristics were improved in the TF treatment groups. (Figure 1A) As shown by hematoxylin and eosin (HE) staining and Masson staining, rats in the blank control group had

complete hepatic lobular structures, normal hepatic cords, and neatly arranged hepatocytes; the hepatocytes were radially arranged in plates around the central vein, with uniform cytoplasm; there was no degeneration, necrosis, inflammatory cell infiltration, or fibrous tissue hyperplasia. In the model group, the hepatic lobules were damaged with obvious fibrous tissue hyperplasia, the arrangement of hepatocyte cords was disordered, pseudolobules had formed in some samples, fibrotic morphology was seen in liver tissue, and fatty degeneration of liver cells was

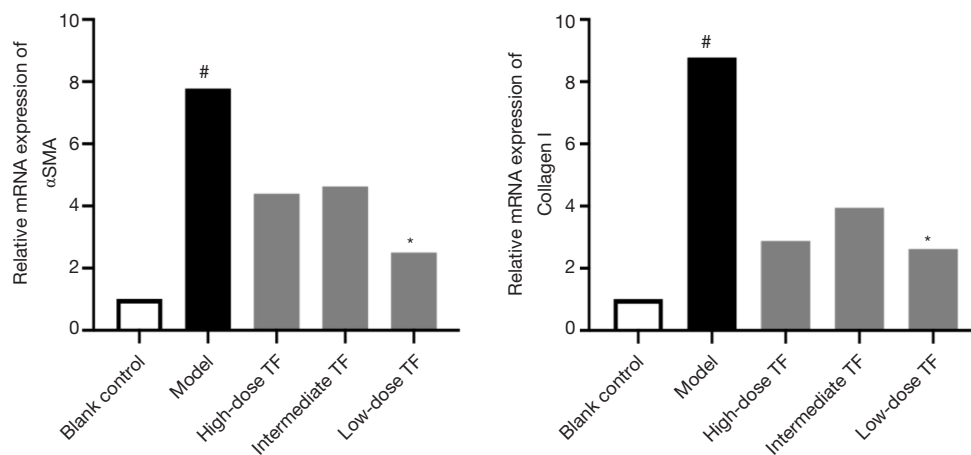


Figure 2 Relative mRNA expressions of α SMA and collagen I in the five groups. #, $P < 0.05$, compared with normal group; *, $P < 0.05$, compared with model group.

visible along with different degrees of liver necrosis and massive infiltration of inflammatory cells. These findings, along with the results of the serum biochemical indicator measurement, suggested that the liver fibrosis models were successfully established. In the TF groups, liver fibroplasia was decreased, liver cell degeneration and necrosis were remarkably reduced, hepatocyte cords were arranged relatively regularly, the pseudolobules were reduced, and the inflammatory cell infiltration was significantly decreased (Figure 1B,C).

Decreased mRNA expression of cytokines related to liver fibrosis

After the therapeutic effects were confirmed, we further investigated the expressions of α SMA, a marker of hepatic stellate cell (HSC) activation, and collagen 1, the main component of ECM. The results showed that the mRNA expressions of α SMA and collagen 1 were significantly higher in the model group than in the blank control group and significantly lower in the TF groups than in the model group (Figure 2).

Significantly decreased expressions of cytokines related to liver fibrosis

After the therapeutic effects were confirmed, we further investigated the expressions of α SMA, a marker of HSC activation, and collagen 1, the main component of ECM in liver tissue. The results showed that the expressions of α SMA and Collagen 1 were significantly higher in the model group than in the blank control group and

significantly lower in the TF groups than in the model group (Figure 3).

Differentially expressed proteins caused by TF treatment

Proteomics analysis showed that a total of 5,014 proteins were identified during the experiment, among which 205 proteins were differentially expressed with significance. Compared with the model group, the expressions of 77 proteins were up-regulated and those of 128 proteins were down-regulated in the TF groups. Proteins that were significantly differentially expressed included AOX, Idil, ADH, FABP, and von Willebrand factor (vWF). Some of the differentially expressed proteins are shown in Table 2. We selected FABP and vWF, which are closely related to liver fibrosis, for subsequent tests.

To understand the biological role of the differentially expressed proteins, we performed GO functional annotation analysis of the differentially expressed proteins in terms of biological processes, cellular components, and molecular function. As shown by the GO function annotation analysis (Figure 4A), the differential proteins were mainly involved in nine biological processes including the cellular process (17%), single organism process (17%), metabolic process (15%), and biological regulation (10%). For the “cellular component”, the differentially expressed proteins mainly were mainly involved in the cell (28%), organelle (25%), membrane (13%), and extracellular regions (13%). The molecular functions of the differentially expressed proteins included binding (48%), catalytic activity (35%), and

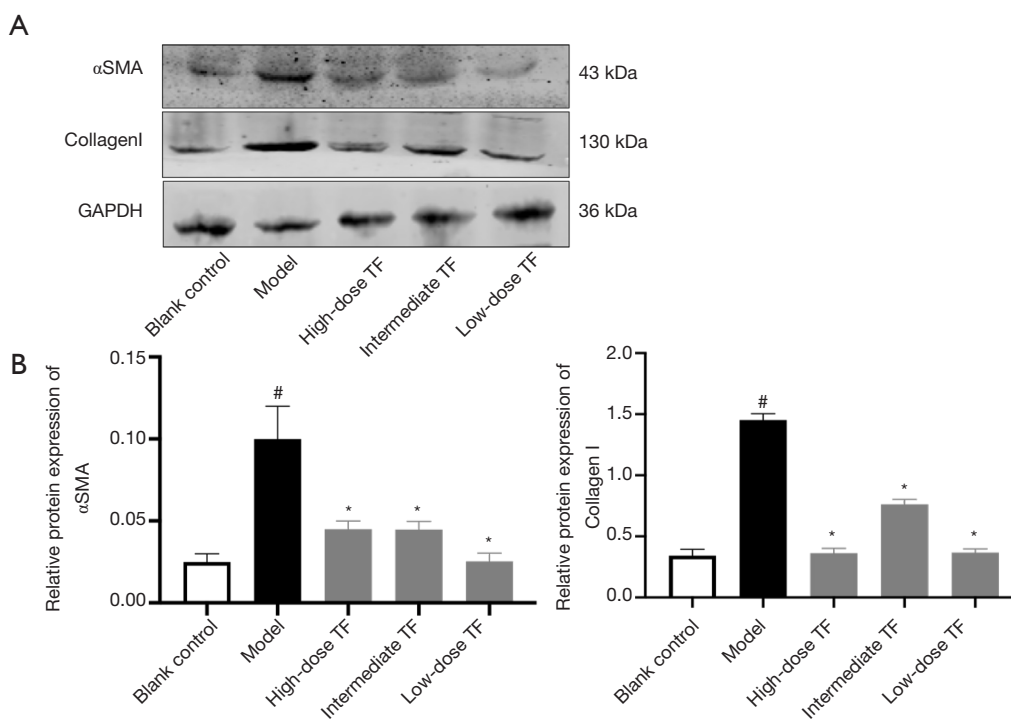


Figure 3 Western blot detection results. (A) Effects of total flavonoids from *Scabiosa comosa* Fisch. ex Roem. et Schult. on the expressions of α SMA and collagen I; (B) the values of the band intensity represent the densitometric estimation of each band normalized by GAPDH in A. #, $P < 0.05$, compared with the blank control group; *, $P < 0.05$, compared with the model group.

structural molecule activity (6%). Subcellular location showed that the majority of the differentially expressed proteins were located in the cytoplasm (47%), followed by mitochondria (17%), and ECM (12%) (Figure 4A). Analysis of the signaling pathways participated by the differentially expressed proteins can help to determine the major signaling pathways involved by these proteins, elucidate their biological functions, and provide a theoretical basis for further research.

KEGG pathway analysis indicated that the differentially expressed proteins were mainly involved in nitrogen metabolism, histamine metabolism, primary bile acid biosynthesis, drug metabolism (synthesis of cytochrome P450 enzymes), and retinol metabolism (Figure 4B). Compared with the model group, the down-regulated proteins in the TF groups were mainly involved in vitamin B6 metabolism, bile secretion, JAK-STAT signaling pathway, and peroxisome proliferator activated receptor (PPAR) signaling pathway. We selected the PPAR and ECM receptor interaction pathways that are closely related to liver fibrosis for further research. The KEGG pathway maps are shown in Figure 5.

Verification of the possible targets and pathways of TF treatment for liver fibrosis

According to the results of KEGG analysis, the down-regulated proteins were further verified with WB (Figure 6). Compared with the model group, the expressions levels of FABP and vWF significantly decreased in TF groups, which were consistent with the proteomic findings.

Discussion

Liver fibrosis is caused by chronic hepatitis B virus or hepatitis C virus infection, alcohol abuse, non-alcoholic fatty liver disease, and other relatively rare diseases. Occurring at the end stage of progressive liver fibrosis, cirrhosis affects 1–2% of the global population and causes more than one million deaths worldwide each year. Thus, timely and effective treatment of liver fibrosis in its early stages is urgent needed. At present, there is no ideal medical treatment for liver fibrosis. The armamentarium of both traditional Chinese medicine and traditional Mongolian medicine contain a vast and varied collection of medicinal

Table 2 Selected differentially expressed proteins

| Protein ace accession | Gene | Regulated | TF/MC P value |
|-----------------------|---------------------|-----------|---------------|
| A0A096MJY6 | <i>Gbe1</i> | Up | 0.0023001 |
| A0A0A0MY01 | <i>Fabp2</i> | Down | 0.030736 |
| A0A0A0MY22 | <i>Siae</i> | Down | 0.00008242 |
| A0A0G2JSR1 | <i>LOC100911881</i> | Down | 0.000099779 |
| A0A0G2JST6 | <i>Hk3</i> | Down | 0.0147249 |
| A0A0G2JSV6 | <i>Hba-a2</i> | Up | 0.00166202 |
| A0A0G2JUA5 | <i>Ahnak</i> | Down | 1.62E-12 |
| A0A0G2JV79 | <i>Slco2a1</i> | Up | 0.0037221 |
| A0A0G2JVG3 | <i>Pkm</i> | Down | 0.0031209 |
| A0A0G2JWK7 | <i>Tagln</i> | Down | 1.85E-12 |
| A0A0G2JZB6 | - | Up | 0.007105 |
| A0A0G2K0Q7 | <i>Mylk</i> | Down | 1.00E-32 |
| A0A0G2K1R4 | <i>Rdh5</i> | Up | 0.00162316 |
| A0A0G2K1Z5 | <i>Aox3</i> | Down | 8.88E-16 |
| A0A0G2K531 | <i>Gpx3</i> | Down | 4.84E-09 |
| A0A0G2K588 | <i>Ltbp4</i> | Down | 0.000076494 |
| A0A0G2K890 | <i>Ezr</i> | Down | 0.000061858 |
| A0A0H2UHF8 | <i>Orm1</i> | Down | 0.0015579 |
| A0A0H2UHH9 | <i>Rps24</i> | Up | 0.00160188 |
| A0A0H2UHL6 | <i>Ctsh</i> | Up | 7.30E-07 |
| A0A0H2UHN2 | <i>Idi1</i> | Down | 7.01E-09 |
| A0A0H2UI07 | <i>Pklr</i> | Up | 1.62E-12 |
| A1A5Q1 | <i>Parp9</i> | Down | 0.0002447 |
| A1L128 | <i>Adh4</i> | Up | 0.007061 |
| B0BMT9 | <i>Sqor</i> | Down | 0.00082278 |
| B0BNA5 | <i>Cotl1</i> | Down | 0.000041097 |
| B0BNJ1 | <i>Sri</i> | Down | 1.55E-15 |
| B0BNN3 | <i>Ca1</i> | Up | 1.00E-32 |
| B0K031 | <i>Rpl7</i> | Down | 1.06E-11 |
| B2GUZ3 | <i>Mthfd1l</i> | Down | 0.0033616 |
| B2RZ37 | <i>Reep5</i> | Down | 1.22E-06 |
| B2RZD4 | <i>Rpl34</i> | Down | 0.00000455 |
| B4F7E8 | <i>Fam129b</i> | Down | 0.00019703 |
| B5DFN3 | <i>Uqcc2</i> | Up | 0.00045992 |

Table 2 (continued)

Table 2 (continued)

| Protein ace accession | Gene | Regulated | TF/MC P value |
|-----------------------|---------------------|-----------|---------------|
| C0JPT7 | <i>Flna</i> | Down | 9.73E-08 |
| D3Z8I7 | <i>Gstt3</i> | Down | 0.0130191 |
| D3Z8X6 | <i>Dtx3l</i> | Down | 2.10E-09 |
| D3Z952 | <i>Mfap2</i> | Down | 0.0075019 |
| D3ZAP3 | <i>Map10</i> | Up | 0.0042555 |
| D3ZH41 | <i>Ckap4</i> | Down | 5.12E-12 |
| D3ZNJ5 | <i>Inmt</i> | Up | 3.78E-09 |
| D3ZUB0 | <i>Rcn1</i> | Down | 1.52E-06 |
| D3ZV82 | <i>LOC685067</i> | Down | 0.00060362 |
| D4A2F1 | <i>Agrn</i> | Down | 0.00040078 |
| D4A5K9 | <i>Gys2</i> | Up | 4.24E-10 |
| D4A6W6 | - | Down | 0.0194623 |
| D4A7N7 | <i>Ttc39d</i> | Up | 2.03E-12 |
| D4A9A3 | <i>Cenpv</i> | Up | 3.77E-11 |
| D4AAV1 | <i>Amdhd1</i> | Up | 3.12E-10 |
| D4ACN7 | <i>Myof</i> | Down | 0.044516 |
| D4AEH9 | <i>Agl</i> | Up | 1.00E-32 |
| F1LM03 | <i>LOC100361492</i> | Down | 0.00063668 |
| F1LNF0 | <i>Myh14</i> | Down | 0.00097815 |
| F1LPR6 | - | Down | 0.00056308 |
| F1LQN3 | <i>Rtn4</i> | Down | 0.000040023 |
| F1LR02 | <i>Col18a1</i> | Down | 1.23E-06 |
| F1LRQ1 | <i>Aox1</i> | Down | 1.00E-32 |
| F1LUV9 | <i>Ncam1</i> | Down | 0.0085628 |
| F1LXN6 | <i>Slc28a2</i> | Down | 0.00080229 |
| F1LZF4 | <i>Col6a5</i> | Down | 0.0068402 |
| F1LZJ4 | <i>Hyi</i> | Up | 3.16E-14 |
| F1M5L5 | --- | Up | 0.0159627 |
| F1M6F4 | --- | Up | 0.00026453 |
| F1M7N8 | <i>Ugt2b37</i> | Up | 0.0049027 |
| F1M7S4 | <i>Cpa3</i> | Down | 5.81E-07 |
| F1M957 | <i>Vwf</i> | Down | 0.000002193 |
| F1MAC0 | <i>Ifi47</i> | Down | 2.68E-06 |
| P62738 | <i>Acta</i> | Down | 0.0053201 |

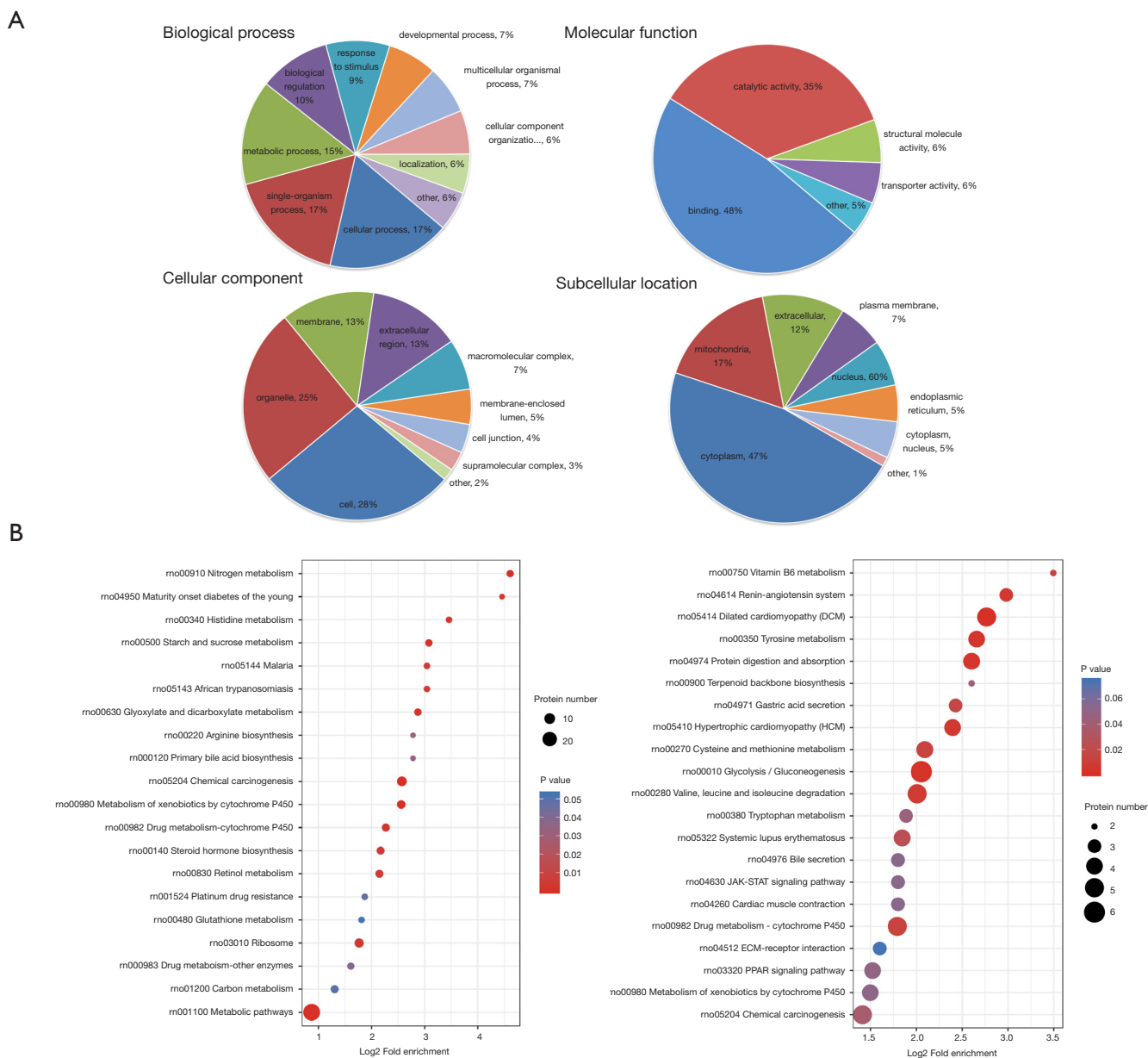


Figure 4 Proteomics results. (A) Go function annotation of differentially expressed proteins and subcellular localization; (B) KEGG enrichment analysis for the comparisons of up-regulated and down-regulated proteins between model group and TF groups.

plants. While some herbs have shown good effectiveness in treating chronic liver diseases including liver fibrosis, no specific and objective markers of liver fibrosis or randomized controlled trials are available; as a result, the roles of these herbs in treating liver fibrosis have not been widely recognized.

In our current study, rat models of hepatic fibrosis were established to explore the role of TF from *Scabiosa*

comosa Fisch. ex Roem. et Schult. in treating liver fibrosis by observing the pathology and morphology of the livers, detecting the changes in liver function indicators, measuring the content of hydroxyproline, and determining the α SMA and collagen I expression levels in liver tissue (9). Both ALT and AST are non-specific intracellular functional enzymes, while ALP is responsible for hydrolysis of phosphomonoesters in liver cells. The levels of these three

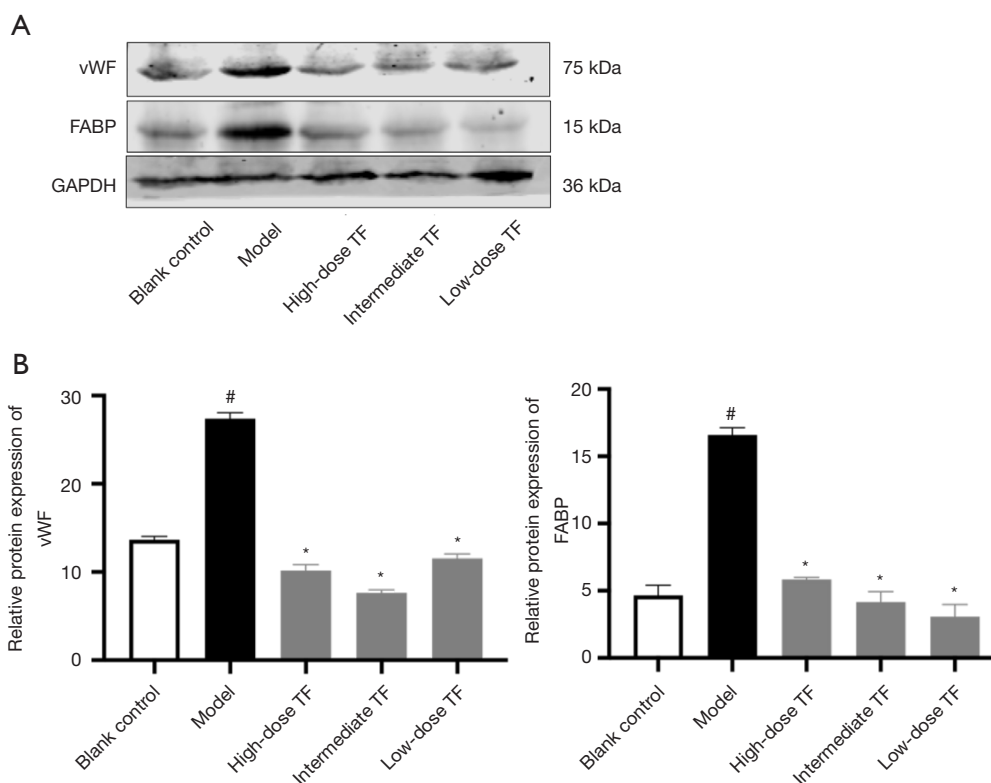


Figure 6 Differential protein western blot detection results. (A) Effects of TF from *Scabiosa comosa Fisch. ex Roem. et Schult.* on the protein expressions of FABP and vWF; (B) the value of the band intensity represents the densitometric estimation of each band normalized by GAPDH in A. #, $P < 0.05$, compared with the blank control group; *, $P < 0.05$, compared with the model group.

indicators are low in normal serum; however, the serum levels of these three markers increase when liver cells are damaged and the permeability of the liver cell membrane is increased. Therefore, they are good indicators of liver cell death and liver inflammation. Liver histopathology allows the direct observation of the histopathological changes and thus is the gold standard for judging the presence of fibrosis and its severity. In our current study, the liver function markers including ALT, AST, and ALP were significantly higher in the model group than in the blank control group, and demonstrated obvious pathological changes of liver fibrosis. Compared with the model group, the TF groups had significantly decreased ALT, AST, and ALP, along with obviously improved pathological findings of liver fibrosis, suggesting TF has a therapeutic effect on liver fibrosis. Furthermore, we determined the mRNA and protein expressions of α SMA and collagen I in liver tissue, and the results showed that these expressions were significantly higher in the model group than in the blank control group and more significantly decreased in

the TF groups than in the model group. Collagen is the most abundant protein in mammals. As the major fibrous protein in the ECM, it plays a key role in the deposition of pathological matrix during liver fibrosis, and its level increases with the progress of fibrosis (10-12). Meanwhile, α SMA is a member of the actin family. A key link in the development of liver fibrosis consists of cytokines in the liver activating HSC through a variety of cell signaling pathways to cause them to proliferate and migrate, which results in the massive secretion of ECM and the expression of α SMA with contractile function. Thus, positive α SMA expression is a marker of HSC activation and liver fibrosis (13,14). In our current study, the α SMA and collagen I expression levels significantly increased in the livers of rats with carbon tetrachloride-induced liver fibrosis and then significantly decreased after treatment with TF from *Scabiosa comosa Fisch. ex Roem. et Schult.*, suggesting that TF from *Scabiosa comosa Fisch. ex Roem. et Schult.* may suppress liver fibrosis by inhibiting HSC activation and collagen synthesis.

We also performed a quantitative proteomics analysis to fully understand the biological effects of TF from *Scabiosa comosa Fisch. ex Roem. et Schult.* It was found that most of the differentially expressed proteins existed in the cytoplasm and were mainly involved in translation, post-translational modification, signal transduction, energy production and conversion, and lipid transport and metabolism. We selected FABP and vWF, which are related to liver fibrosis, for further study. KEGG pathway analysis indicated that the differentially expressed proteins were involved in nitrogen metabolism, histamine metabolism, primary bile acid biosynthesis, drug metabolism (synthesis of cytochrome P450 enzymes), retinol metabolism, vitamin B6 metabolism, bile secretion, and a variety of liver fibrosis-related signaling pathways including JAK-STAT, PPAR, and ECM receptor interaction. Studies have demonstrated that suppression of JAK-STAT pathway expression can inhibit HSC activation and liver fibrosis (15,16). It has also been found that retinol can protect against liver fibrosis (17).

Based on the differentially expressed proteins and the results of KEGG pathway enrichment analysis, we selected two pathways including ECM receptor interaction and PPAR for further research. ECM is a complex network structure composed of macromolecular substances that are synthesized and secreted by various tissues and cells (e.g., fibroblasts, mesenchymal cells, and epithelial cells) in the body and distributed and aggregated on cell surface and intercellular substances (18). The synthesis of ECM increases, and its degradation decreases during liver fibrosis, leading to excessive deposition of ECM in the liver. HSC is the main source of ECM in liver tissue, and HSC activation and conversion into myofibroblasts are the key links during the onset and progression of liver fibrosis. Changes in ECM during liver fibrosis include the changes in the proportions of various components and the alterations of the molecular and spatial structures, which result in the change of the internal environment of the liver. A series of signaling pathways can lead to the activation, proliferation, contraction, migration, and apoptosis of HSCs, which further aggravate the massive deposition and disturbances of ECM and accelerate the progression of liver fibrosis. Proteomic findings showed that the expressions of vWF and collagen I, two components of ECM, were down-regulated. vWF is a complex receptor glycoprotein whose main physiological role is to bind to and stabilize coagulation factor VIII (19). The expression level of liver vWF is low in healthy individuals, and most of the vWF detected exists in vascular endothelial cells rather than

hepatic sinusoidal endothelial cells. When hepatic fibrosis occurs, sinusoid capillarization will be found in hepatic sinusoidal endothelial cells, and a large number of cells will become vWF-positive (20). Proteomics findings in our current study showed that the vWF content in liver tissue was significantly down-regulated. Thus, vWF may be a potential therapeutic target for TF treatment of liver fibrosis.

PPAR, a member of the ligand-activated nuclear transcription factor superfamily, includes three phenotypes: α , β , and γ (21), and fatty-acid-binding protein (FABP) plays an important role in the relevant lipid-mediated metabolic pathways (22). The blood level of liver-type fatty acid binding protein (L-FABP) is a sensitive enzymatic indicator for early hepatocyte damage, and its specificity and sensitivity are superior to the conventional liver function indicators (23). It has been found that serum L-FABP level is positively correlated with the severity of hepatitis, with the sensitivity and specificity being 75% and 100%, respectively. In recent years, it has been proposed that L-FABP may affect liver fatty acid metabolism by altering the activity or expression level of PPAR- α in the PPAR signaling pathway (24). L-FABP not only directly regulates the metabolism of fatty acids in the liver but also shuttles between cell lipids and the nuclei, where it binds to PPAR α and thus indirectly regulates the transport and absorption of fatty acids in liver cells and maintains lipid homeostasis in liver. Studies have shown that L-FABP can regulate the metabolism of fatty acids in hepatocytes and the utilization of fatty acids in HSCs; also, it can regulate the fibrosis in patients with non-alcoholic fatty liver disease. Proteomics results from the literature indicate that the content of FABP decreased, suggesting that TF from *Scabiosa comosa Fisch. ex Roem. et Schult.* may inhibit FABP expression and protect against liver damage; however, its anti-fibrotic effect needs further investigation (25).

In summary, we demonstrated the anti-fibrotic effect of TF from *Scabiosa comosa Fisch. ex Roem. et Schult.* through multi-dimensional experiments. Furthermore, quantitative proteomics technology revealed that TF exerted its effect via multiple pathways and on multiple targets: we can speculate that ECM receptor interaction and PPAR were the possible action pathways, whereas α SMA, collagen I, FABP, and vWF may be the potential targets. Thus, our study provides reliable experimental data for exploring the mechanism of the anti-fibrosis effect of TF from *Scabiosa comosa Fisch. ex Roem. et Schult.* and extracting effective anti-fibrotic compounds.

Acknowledgments

Funding: Supported by the National Natural Science Foundation of China (No. 81560706 and No. 81960759), the Inner Mongolia Natural Science Foundation (No. 2014MS0841 and No. 2019MS08010), the Inner Mongolia Young Innovative Talents Training Program, and the Inner Mongolia Medical University Talent Team Program.

Footnotes

Conflicts of Interest: The authors have no conflicts of interest to declare.

Ethical Statement: The authors are accountable for all aspects of the work in ensuring that questions related to the accuracy or integrity of any part of the work are appropriately investigated and resolved.

Open Access Statement: This is an Open Access article distributed in accordance with the Creative Commons Attribution-NonCommercial-NoDerivs 4.0 International License (CC BY-NC-ND 4.0), which permits the non-commercial replication and distribution of the article with the strict proviso that no changes or edits are made and the original work is properly cited (including links to both the formal publication through the relevant DOI and the license). See: <https://creativecommons.org/licenses/by-nc-nd/4.0/>.

References

- Lopez-Lopez V, Robles-Campos R, Brusadin R, et al. ALPPS for hepatocarcinoma under cirrhosis: a feasible alternative to portal vein embolization. *Ann Transl Med* 2019;7:691.
- Li T, Che-Nordin N, Wang YX, et al. Intravoxel incoherent motion derived liver perfusion/diffusion readouts can be reliable biomarker for the detection of viral hepatitis B induced liver fibrosis. *Quant Imaging Med Surg* 2019;9:371-85.
- Xu XW, Luo SQ, Liu LL. Pilot test of chemical component of *Scabiosa comosa* Fisch. ex Roem. et Schult. *Silicon Valley* 2008;12:3-4.
- Ruzzenente A, De Angelis M, Conci S, et al. The albumin-bilirubin score stratifies the outcomes of Child-Pugh class A patients after resection of hepatocellular carcinoma. *Transl Cancer Res* 2019;8:S233-44.0
- Bai YF, Zhou XM, Zhou CF, et al. Isolation, identification and determination of the active compounds in *Scabiosa comosa* Fisch. *Northwest Pharmaceutical Journal* 2014;29:564-6.
- Yang HX, Dong MX, Mi YQ, et al. Effect of Mongolia scabiosus acid on serum MMP -1 and TIMP -1 expression levels in experimental liver fibrosis rats. *China Pharmaceuticals* 2014;23:37-8.
- Bai YF, Alatanqige, Li DL, et al. Protection and immune regulation of Mongolia scabiosus acid on autoimmune hepatitis. *Journal of Medicine and Pharmacy of Chinese Minorities* 2007;04:44.
- Ma YH, Duan S, Jin R, et al. Study on the anti-hepatic fibrosis effect of Mongolian Medicine Erigen-7 in rats. *Journal of Inner Mongolia University (Natural Science Edition)* 2016;47:526-32.
- Xu L, Yin L, Tao X, et al. Dioscin, a potent ITGA5 inhibitor, reduces the synthesis of collagen against liver fibrosis: Insights from SILAC-based proteomics analysis. *Food Chem Toxicol* 2017;107:318-28.
- Vahdati Hassani F, Abnous K, Mehri S, et al. Proteomics and phosphoproteomics analysis of liver in male rats exposed to bisphenol A: Mechanism of hepatotoxicity and biomarker discovery. *Food Chem Toxicol* 2018;112:26-38.
- Li X, Li Z, Zhao W, Qin J. Effect of high fat diet on proteome in mice stomachs]. *Sheng Wu Gong Cheng Xue Bao* 2018;34:1840-9.
- Nurmik M, Ullmann P, Rodriguez F, Haan S, Letellier E. In search of definitions: Cancer-associated fibroblasts and their markers. *Int J Cancer* 2020;146:895-905.
- Zeisberg M, Kalluri R. Cellular mechanisms of tissue fibrosis. 1. Common and organ-specific mechanisms associated with tissue fibrosis. *Am J Physiol Cell Physiol* 2013;304:C216-25.
- Higashi T, Friedman SL, Hoshida Y. Hepatic stellate cells as key target in liver fibrosis. *Adv Drug Deliv Rev* 2017;121:27-42.
- Dodgington DW, Desai HR, Woo M. JAK/STAT - Emerging Players in Metabolism. *Trends Endocrinol Metab* 2018;29:55-65.
- Gao YQ, Su D, Zhang HH. Research advances in traditional Chinese medicine in interfering JAK/STAT signaling pathway. *Shizheng Traditional Chinese Medicine* 2018;29:2236-40.
- Romeo S, Valenti L. Regulation of retinol-binding protein 4 and retinol metabolism in fatty liver disease. *Hepatology* 2016;64:1414-6.
- Qin YM, Chen SH. Influence of extracellular matrix on hepatic stellate cells during liver fibrosis process. *Journal*

- of Practical Hepatology 2017;20:381-4.
19. Liu SN, Liu HM, Zhou HY, et al. Effect of Qizhu Granules on vWF and Caveolin-1 expression of hepatic sinus endothelium cells in rat with hepatic fibrosis model. *Beijing Journal of Traditional Chinese Medicine* 2019;38:230-3+305.
 20. Hu CH, Luo J, Li JJ. Changes and significance of serum SOD and VWF levels in patients with liver cirrhosis. *Modern Diagnosis and Treatment* 2015;26:2594-6.
 21. Hostetler HA, McIntosh AL, Atshaves BP, et al. L-FABP directly interacts with PPARalpha in cultured primary hepatocytes. *J Lipid Res* 2009;50:1663-75.
 22. Zhang Y. Roles of CBR1 and FABP1 in bifendate treatment of liver fibrosis in rats. Hebei Medical University, 2015.
 23. Zhang Z, Fu WJ, Xing YF, et al. Research advances in the relationship between L-FABP/PPAR α signaling pathway and non-alcoholic steatohepatitis. *Shandong Medical Journal* 2016;56:98-100.
 24. Akbal E, Köklü S, Koçak E, et al. Liver fatty acid-binding protein is a diagnostic marker to detect liver injury due to chronic hepatitis C infection. *Arch Med Res* 2013;44:34-8.
 25. Chen A, Tang Y, Davis V, et al. Liver fatty acid binding protein (L-Fabp) modulates murine stellate cell activation and diet-induced nonalcoholic fatty liver disease. *Hepatology* 2013;57:2202-12.

Cite this article as: Menggensilimu, Yuan H, Zhao C, Bao X, Wang H, Liang J, Yan Y, Zhang C, Jin R, Ma L, Zhang J, Su X, Ma Y. Anti-hepatic fibrosis effect of total flavonoids from *Scabiosa comosa* Fisch. ex Roem. et Schult. on liver fibrosis in rat models and its proteomics analysis. *Ann Palliat Med* 2020;9(2):272-285. doi: 10.21037/apm.2020.02.29